Final report dated July 2021

Demonstration of Energetic Potential, Safety and regulatory compliance of Airborne Wind Energy Systems in Switzerland on a pilot scale

Source: ©TwingTec 2020

Date: July 2021

Location: Bern

Authors:
Corey Houle, TwingTec AG, corey.houle@twingtec.ch
Rolf Luchsinger, TwingTec AG, rolf.luchsinger@twingtec.ch

SFOE project coordinators:
Men Wirz, men.wirz@bfe.admin.ch
Katja Maus, katja.maus@bfe.admin.ch
Lionel Perret, lionel.perret@planair.ch

The authors bear the entire responsibility for the content of this report and for the conclusions drawn therefrom.

This project was performed in coordination with Skypull SA, another Swiss-based developer of Airborne Wind Energy systems.

Zusammenfassung

Abschlussbericht über die Aktivitäten von TwingTec und die wichtigsten Ergebnisse des Projekts: „Nachweis des energetischen Potenzials, der Sicherheit und der Einhaltung der gesetzlichen Vorschriften von Airborne Wind Energy Systemen (AWE) in der Schweiz im Pilotmaßstab.“

Im Verlauf des Projekts haben wir die Sichtbarkeit des Systems für andere Luftraumbenutzer sowie verschiedene Verfahren zur Minimierung des Luftrisikos untersucht um die Wahrscheinlichkeit einer Kollision mit bemannten Flugzeugen auf ein akzeptables Maß zu reduzieren. Der gewählte Ansatz wurde durch Flugtests und mittels Rückmeldungen des BAZLs validiert und im Rahmen der AWEurope Arbeitsgruppe zum Thema Sicherheit an die AWE-Community weitergegeben.

Akustische Messungen sowie Messungen der produzierten Leistung wurden mittels Schlepp- und Windtests durchgeführt. Die Charakterisierung der akustischen Emissionen des Systems wurde mit einem Array von Mikrofonen erreicht. Dies hat zu einer ersten Schätzung der typischen einzuhaltenden Abstände des Systems zu Bauten auf Basis der Schweizer Lärmnormen geführt. LIDAR-basierte Windgeschwindigkeitsmessungen wurden während der Windtests ebenfalls durchgeführt.

Diese Aktivitäten wurden mit dem Pilotsystem von TwingTec durchgeführt, das im Rahmen dieses Projektes weiterentwickelt wurde.

Résumé

Rapport final d'activités de TwingTec et résultats majeurs du projet: "Démonstration du potentiel énergétique, de la sécurité et de la conformité aux règlementations de systèmes Airborne Wind Energy (AWE – énergie éolienne aéroportée) en Suisse à l'échelle d'un pilote".
Au cours de ce projet, nous avons examiné la visibilité du système pour les autre usagés de l'espace aérien ainsi que les différentes procédures visant à réduire à un niveau acceptable les risques de collision avec un aéronef piloté. Cette approche a été validée avec des essais en vol et la collaboration de l'OFAC, puis diffusée à la communauté AWE par l'intermédiaire du groupe de travail AWEurope en charge du thème de la sécurité.
Des mesures acoustiques et des mesures de performance ont été réalisées pendant des essais tractés (vent simulé) et des essais en conditions réelles (vent). Les émissions acoustiques du système ont été caractérisées grâce à un ensemble de microphones. Cela a permis d'estimer des distances d'éloignement basées sur les réglementations suisses sur le bruit. Des mesures de vitesse de vent ont également été effectuées avec un LIDAR pendant des essais en conditions réelles.
Ces activités ont été réalisées avec le système pilote de TwingTec, dont le développement a été poursuivi au cours de ce projet.

Summary

Final report on TwingTec's activities and key results of the project: "Demonstration of energetic potential, safety and regulatory compliance of Airborne Wind Energy Systems (AWE) in Switzerland on a pilot scale."

During the course of the project we have investigated the visibility of the system for other airspace users as well as the various air risk mitigations procedures that can be applied to reduce the chance of

a collision with manned aircraft to acceptable levels. This approach has been validated through flight tests, feedback from FOCA and disseminated to the AWE community as part of the AWEurope Working Group on the topic of safety.

Acoustic and power performance measurements were performed during both tow and wind tests. A characterization of the acoustic emissions of the system was achieved with an array of microphones. This has led to an estimate of typical standoff distances based on Swiss Noise standards. LIDAR based wind speed measurements during wind tests were also performed.

These activities have been performed with TwingTec`s pilot system, which has been further developed during the course of this project.

Main findings

Visibility of AWE systems for airspace users

- Visibility of AWE systems for airspace users can be maximized with the following actions:
    - Appropriate marking and lighting on the aircraft
    - Use of a FLARM system with Ground Alert Zone function
    - Publication of Danger Zone via NOTAM
- Distance at which the system is visible to an incoming aircraft varies on many factors, but has been estimated to be about 1km for TwingTec's pilot aircraft with a wing span of 5.5m under clear conditions based on a literature study.
- Visible distance will increase as the systems become larger (linear to wingspan based on results of a literature study) and under clear conditions TwingTec`s product concept TT1000 (rated output of 1000kW), with a wingspan of 30m, should be visible from a distance of at least 5km.

Performance measurements

- Performance of the system was measured during two sets of tests: tow tests in which the wing is pulled by a truck in order to create a controlled wind environment and during wind tests where the system is flown at a test site during a windy day.
- During tow tests the system performance could be very accurately measured due to the low uncertainty over the wind speed. The results were used to validate a dynamic system simulation which predicts that the system mechanical power target is achievable.
- LIDAR measurements were performed during wind tests which allowed the wind speed at operating altitude to be calculated and compared against the measured system performance.

Acoustic characterization

- Acoustic measurements were performed during tow tests using an array of microphones and the measurements of relative distance to the wing with a GPS.
- A linear relationship between the airspeed and the acoustic power emissions of the wing were identified, which leads to a methodology for the estimation of minimum distances according to Swiss standards.
- A first estimate of minimum standoff distances has been made but further investigations are needed before making any conclusions.

Contents

Abbreviations

All abbreviations have been explained in the text.

1 Introduction

1.1 Background information and current situation

- The airborne wind energy sector continues to develop and first commercial products in the range of 100kW utilizing soft kites are being announced.

- A number of joint activities have been carried out over the last year organized by Airborne Wind Europe (industry group) as well as FGW in the creation of technical guidelines for AWE.

- A specific AWE task has been proposed as part of IEA wind TEM#102, with a focus on 5 areas:
  - Resource potential and markets
  - Reference models, tools and metrics
  - Safety and regulation
  - Social acceptance
  - AWES architecture

- American company Makani (funded by Google) have wrapped up their activities in early 2020 and released a significant amount of documentation as well as videos (and a feature length film) from their project which is available here.

- An airborne wind energy conference (AWEC 2021) was planned for September 2021 at Politecnico Milano but has been postponed to June 2022 due to COVID.

1.2 Purpose of the project

The goal of the project is to demonstrate the operation of a small-scale pilot system as well as to investigate relevant topics to the safe and economic operation of AWE. The validation of energetic potential and the development of a roadmap to address key challenges to the commercial operation of AWE systems from a regulatory and permitting perspective was planned in order to show that the technology is ready for larger scale demonstration.

From the perspective of the airspace regulators (like FOCA) it is important to see the technology in action (even at a small scale) before investing too much time in the discussion about regulatory compliance for commercial operations. Also, for de-risking the up scaling towards large demonstration systems it is important that basic functionality and flight maneuvers are proven before the design of the larger systems are finalized.

1.3 Objectives

A number of performance, efficiency and automation targets have been established and investigated during the course of the project.

Additional success controls have been setup concerning the regulatory / permitting aspects:

- Distance at which the system becomes visible to aircraft
- Functionality of FLARM collision avoidance system confirmed
- Noise emissions from the system characterized
- Performance of the system characterized with LIDAR measurements

2   Description of facility

The pilot system is shown below during a hover test (left) and during wind tests (right) at a test site in Switzerland. The system consists of a ground station (GS3) which is mounted on the back of a truck and includes a winch, a battery and a platform from which the Twing can launch and land. The Twing (T29) has been developed over the past year and went through first full-system tow-tests in December 2019 and flew in wind for the first time in February 2020.

Figure 1: T29 launching from GS3 (left). T29 perched on GS3 platform (right).

the flight the pilot and operator are inside the command and control area (top right) where they have a good overview of the system. A power and communication cable connects the ground station to the command area. A wind mast is installed next to the ground station as are warning flags for aircraft.

Figure 2: Aerial view of the test setup.

A high-level schematic view of the pilot system is shown in the figure below.
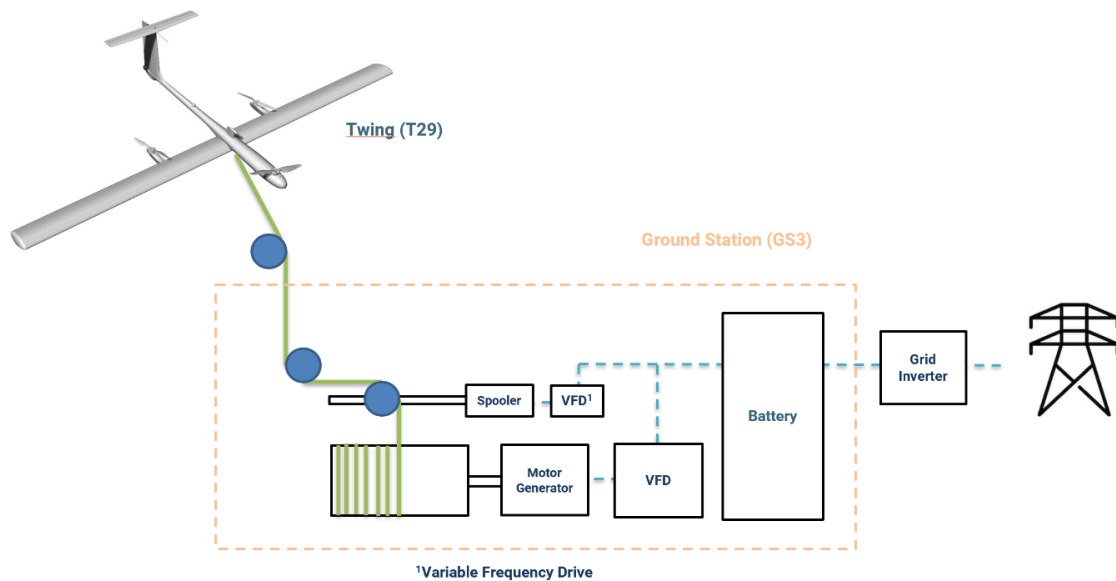
Figure 3: Pilot system Schematic.

Some high level system specifications have been included in the table below.

Parameter	Value
Twing (T29)	
Wingspan	5.5 m
Mass	25 kg
Area	2 m2
Nominal wing loading	3 kN
Ground Station (GS3)	
Generator power	30 kW
Nominal tether force	3 kN
Tether length	300 m
Battery capacity	10 kWh
Mass	1000 kg

A few pictures of the system during testing in November 2020 are shown below:

Figure 4: T29 ready for installation on platform

Figure 5: Command and control center

Figure 6: System ready for launch

3   Procedures and methodology

Performance tests with LIDAR:

During flight testing in Nov. 2020 we could use a LIDAR system provided by Meteotest shown in the picture below.

Model	Windcube V2
Manufacturer	Leosphere / Vaisala
Measurement	Pulsed
Data provided	Wind speed, wind direction, rubulence intensity, vertical wind speed, data availability
Measuring range	40-200m (V2.1 to 300m)
Extended height range	290m (V2.1 to 400m)
# heights	Up to 12
Probe length	20m
Sampling rate	1 hz
Averaging rate	1 second / 1, 2, 5, 10 minutes
Scanning angle	28 degrees
Wind range	0-60m/s+
Speed accuracy	0.1 m/s
Speed uncertainty	2-3 %
Direction accuracy	2 degrees

Figure 7: Wincube V2 installed at test site (top), Overview of key specifications (bottom)

The LIDAR was setup approximately 50 m upwind of the ground station. As the Twing operates about 200 m downwind of the ground station, the wind measurements at altitude needed to be propagated downwind in order to be compared with the measurements from the system. A diagram of the measurement setup and propagation scheme are shown in the figure below.
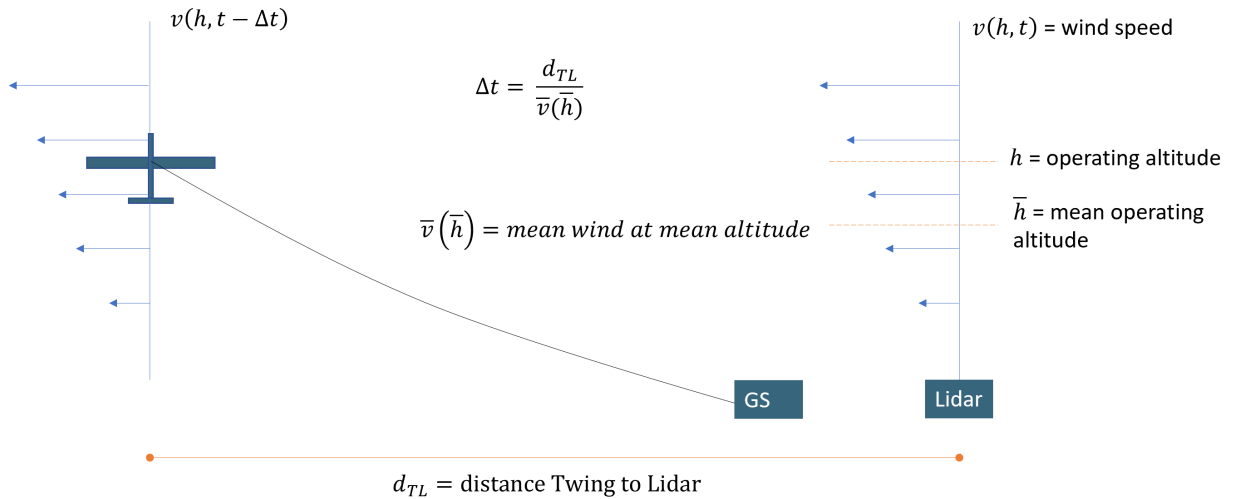
Figure 8: LIDAR measurement setup and propagation scheme

With reference to the figure above, the wind speed at the Twing location from the LIDAR data and GPS position data is calculated as follows:

1. LIDAR provides wind speed measurement at about 1 Hz and every 20m from 40 to 220m height

2. Twing height above ground is measured by GPS

3. LIDAR wind speed on Twing height calculated by linear interpolation along height axis

4. A time shift is introduced in order to account for the spatial distance between LIDAR and Twing

   a. Distance of GS to Twing from the GPS

   b. Another 50m for distance between GS and LIDAR

   c. Assuming constant 10m/s wind speed

There are a number of inaccuracies which are introduced by this method:

- LIDAR measurement does not capture turbulences that are at a smaller scale than the distance between the scanning beams at the respective height -> i.e. at 200m altitude, any fluctuations smaller than about 200m are missed

- Changes in wind speed in the horizontal plane (normal to the wind direction) are not captured

- Actual wind speed changes in time as well as over distance -> error in using a constant wind speed to propagate the measurements

Based on these limitations, we have learned that the use of LIDAR for real-time performance validation is rather challenging and should at least be supplemented with good on-board airspeed / AOA / sideslip measurements. Alternatively, our tow testing method also works quite well for this purpose and is currently our best means of assessing system performance to date.

Validation of LIDAR measurement accuracy:

Regarding the accuracy of the LIDAR measurements, some analysis based on the test results could be performed and will now be presented. A first insight can be taken from a comparison of the LIDAR

measurements taken at the lowest height (40m) compared with measurements form a cup-based anemometer at a height of 4m placed next to the ground station. As expected, the wind speed measured at the mast is mostly lower than measured by the LIDAR as seen in the graphs below.
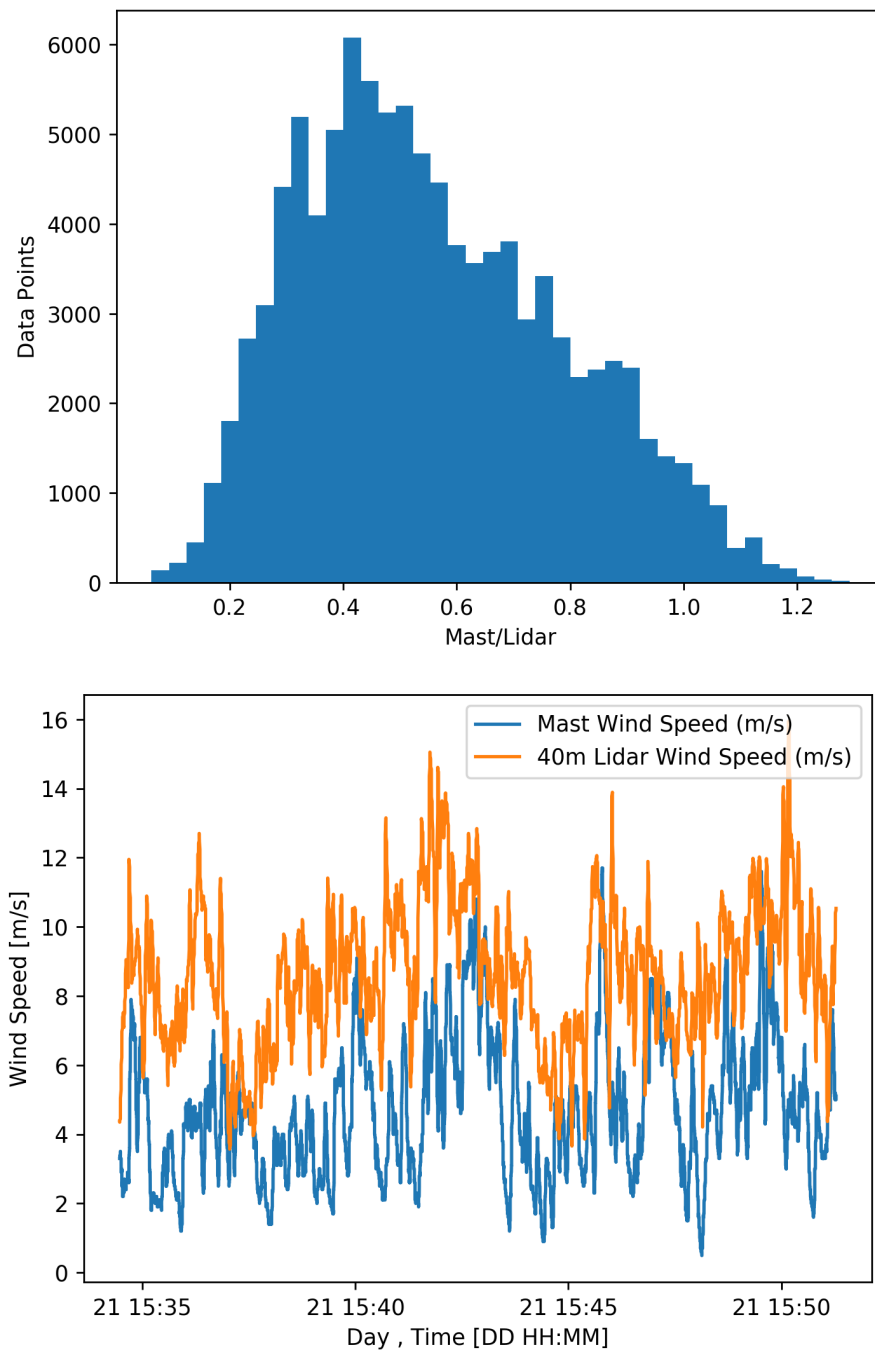

Figure 9: Comparision of wind speed measurements from LIDAR (40m) to mast measurements (4m)

Based on these measurements, a roughness class of 3.0 for the terrain could be calculated based on the logarithmic profile as described here which is typically used for wind profiles below 100m. This is for terrain with the following properties:

Villages, small towns, agricultural land with many or tall sheltering hedgerows, forests and very rough and uneven terrain.

This roughness class is consistent with the type of terrain at the test site as well as the placement of the wind mast relative to the surrounding trees and wind direction.

Some further investigation into the accuracy of the LIDAR based wind measurements could be performed by comparing their values to the airspeed measured by the on-board pitot tube during the retraction phases. A high correlation between the two measurements is expected when the following assumptions are valid:

- Twing flies horizontal and directly into the wind
- Pitot tube is aligned with the wind direction and is unaffected by airflow around the Twing

This is typically the case when the system is in the retraction phase and the vertical speed of the Twing is low. A map of the test site with the flown trajectory shown in blue can be seen in the figure below (top). The two arrows show the direction of the Twing during the retraction phase and the direction from which the wind was blowing (as measured by the LIDAR). Based on this the two measurements are expected to be relatively close.

A comparison of the two measurements for one retraction is shown in the graph below (bottom). As expected, the correlation for most of the retraction is quite good.
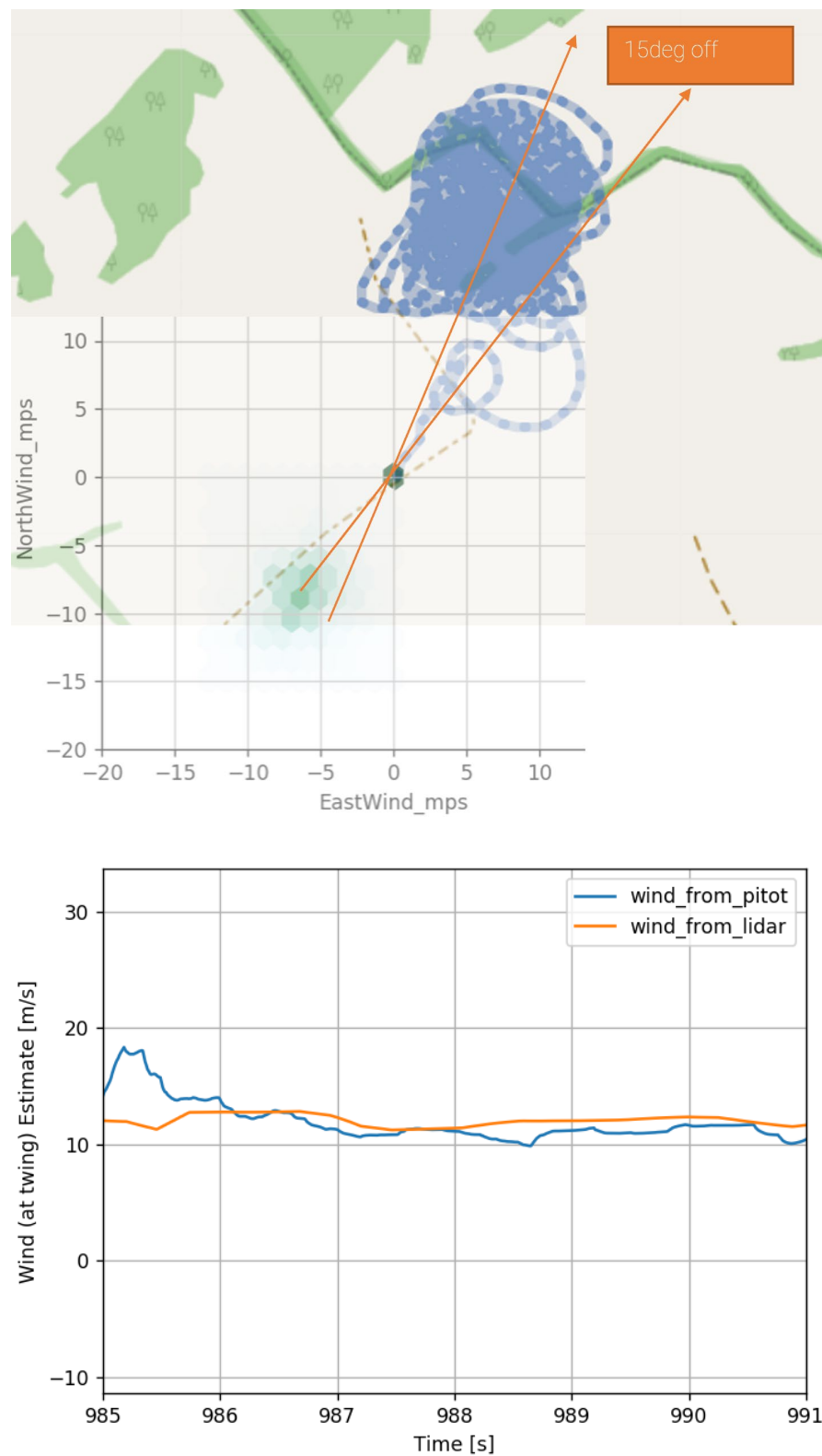
Figure 10: Map of test site showing direction of retraction maneuver vs. wind speed direction (top). Comparison of wind speed estimate from on-board pitot tube vs. LIDAR measurement (bottom)

Evaluation of LIDAR systems for AWE application:

During the course of the project an evaluation of LIDAR systems for the use in AWE measurements was performed. Two other systems were analyzed and compared against the Windcube V2, which was used for the measurements described above. The goal of this analysis was to inform the future purchase of a LIDAR system for use during extended wind testing. An overview of the key specifications of the three systems are include in the table below.

	Windcube V2	**ZX300**	**G250**
Manufacturer	Leosphere / Vaisala	ZX Lidars	Wood Group
Measurement	**Pulsed**	**Continuous wave**	**Pulsed (with 2 axis scanning head)**
Data provided	Wind speed, wind direction, turbulence intensity, vertical wind speed, data availability	Similar to windcube	Horizontal and vertical wind speed and direction, SNR power intensity, local temperature, pressure and relative humidity.
Measuring range	**40-200m (V2.1 to 300m)**	**10-200m**	**45 - 250m**
Extended height range	**290m (V2.1 to 400m)**		**500m**
# heights	Up to 12	Up to 10	15 (in VAD mode)
Probe length	20m	0.7m @ 10m, 7.7m @ 100m	30m (spatial resolution)
Sampling rate	1 hz	50 hz	1 hz (ray update rate)
Averaging rate	1 second / 1, 2, 5, 10 minutes	1 second, 10 minutes	~15 seconds per profile
Scaning angle	28 degrees		
Wind range	0-60m/s+	<1 - 80 m/s	0 - 35 m/s (horizontal)
Speed accuracy	0.1 m/s	0.1 m/s	0.1 m/s (LOS velocity)
Speed uncertainty	2-3 %		
Direction accuracy	2 degrees		
Direction variation		< 0.5 degrees	
Power consumption	**45 W**	**69 W**	**130 - 330 W (temperature dependent)**

		12 V	24V (AC/DC included)
Power input		12 V	24V (AC/DC included)
Dimensions	**L 55 cm, W 56 cm, H 55 cm**	**900 x 900 x 1001 mm**	**L 820mm, W 530mm, H 770mm**
Mass	**46 kg**	**55 kg**	**85 kg (net) / 200 kg with case**
Temperature range	(-)30 - (+)45 degC	(-)40 - (+)50 degC	(-)25 - (+)40 degC
Environmental	IP 67	IP 67	IP66
Measurement reliability under rainy conditions	Windscreen wiper with fluid as standard	Windscreen wiper with fluid as standard	External wash system with fluid as option
Data storage	120 GB (10 years)		480 GB (2 years)
Communication	LAN, USB, 3G, Modbus, Wifi		Ethernet, USB, Remote or Local
Compliance	CE, FCC, ICES		
IEC Classified	Yes: IEC 61400-12.1	Yes: IEC 61400-12.1	Yes: IEC 61400-12.1

Based on analysis of the information presented above a comparison of the three units could be compiled which is shown in the table below.

	Pro`s	Con`s
Windcube V2.1	✓ Measurement height (300m certified / 400m uncertified) ✓ Very user friendly and largest track record in the industry ✓ Smallest size and weight (46kg) ✓ Low power consumption (46W)	✗ Highest price
ZX300	✓ Continuous wave measurement gives profile each second (1hz) as well as lowest measurement height (10m) ✓ Lowest price ✓ Low power consumption (55W)	✗ Measurement height (200m) ✗ Low data availability above max measurement height due to measurement principle ✗ Relatively large (0.9x0.9x1m)
G250	✓ Measurement height (250m certified / 500m uncertified) ✓ Dual axis scanning head allows for measurement of wind flow in a plane which could be interesting for AWE application	✗ Large size and weight (85kg) ✗ High power consumption (110-330W)

Acoustic characterization methodology:

During tow tests with our prototype Twing (T29) we could measure the acoustic emissions with support from acoustics experts at EMPA and correlate them with the airspeed of the Twing, as seen in the figure below. An overview of the positions of the microphones is shown in the figure below.

Tow tests are performed at the airfield in Duebendorf where the ground station is mounted on the back of a truck and driven down the runway to create an artificial wind field. Before starting to drive the Twing is launched using the VTOL system so that it is ready to transition to hover once the "wind speed" created by driving is sufficient. At the end of the runway the Twing transitions back to hover just before the truck stops driving again and it is finally landed. Compared to measuring the acoustic emissions during wind tests this is quite advantageous because the wind speed at the microphones is very low or even zero. Although the moving vehicle does create some additional noise, this is emitted at the ground level and is mostly absorbed by a padded element surrounding the microphone.
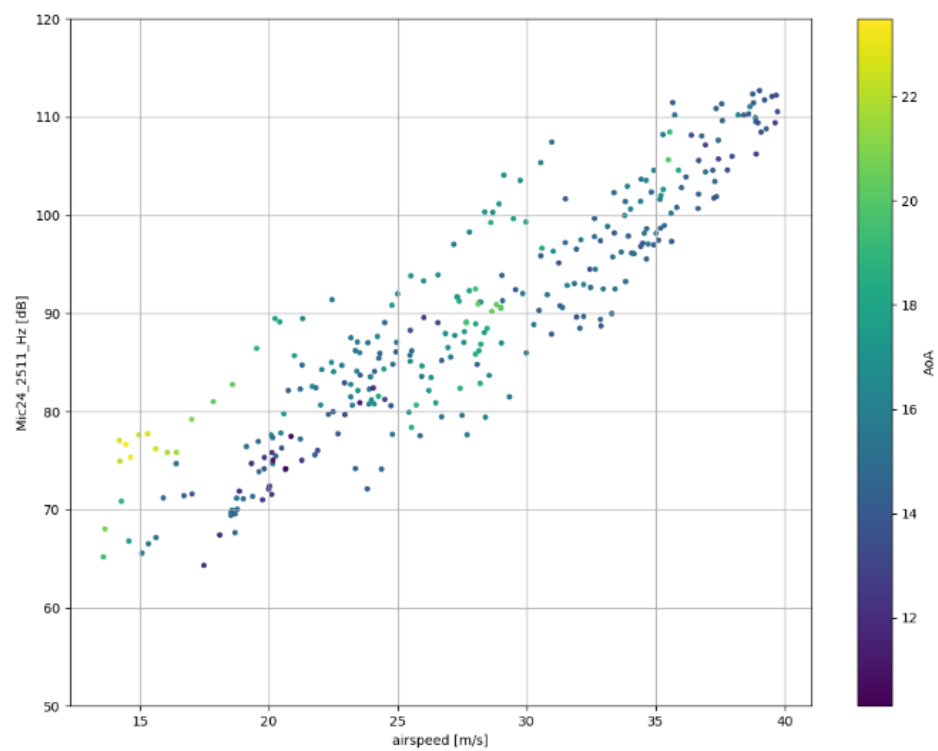
Figure 11: Location of microphones along runway (top). Sounds pressure levels from microphone for 2511 Hz band. (bottom)

4   Results and discussion

Visibility of AWE systems for airspace users

Characterization of AWE system visibility

Two screenshots from a short airborne video of the Twing in operation during flight tests in Nov. 2020 are shown below. The video is taken with a DJI Mavic 2 Pro drone from between 50 and 100 meters away from the Twing. The camera on the drone has a 1" CMOS sensor with 20 million effective pixels and a field of view (FOV) of 77 degrees. The footage was captured at 4K (3840 × 2160 pixels at 25 frames per second) and then post processed to HD (1920 x 1080 pixels). Further specifications can be found here: https://www.dji.com/ch/mavic-2/info#specs

Figure 12: Aerial view of T29

Based on the video of the flight tests alone it is difficult to make an estimate of the distance at which the system will become visible to a pilot. A literature analysis was performed to better understand this topic.

The first study [1] performed a number of flight experiments using two manned aircraft, flying at different orientations towards each other and attempted to quantify the distance at which the `traffic` aircraft becomes visible to the `test` aircraft. An illustration of the experimental conflict scenarios as well as the resulting detection ranges are shown in the figure below. The tests were performed with two piper aircraft, both with a wingspan of about 11m.
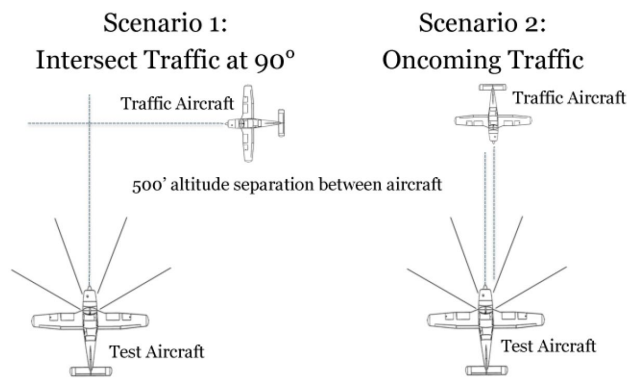
Figure 3.6 – Traffic Aircraft Conflict Scenarios

Table 4.1 - Subject Pilot Detection Ranges

Subject Pilot	Intersect	Oncoming
Pilot 1	1.294	No Detection
Pilot 2	1.178	0.309
Pilot 3	1.898	1.127
Pilot 4	1.710	1.202
Pilot 5	1.167	2.336
Pilot 6	1.773	1.258
Pilot 7	1.559	1.034
Mean	1.511	1.038

(statute miles)

Figure 13: Figures from study in 1. Describing the experiment (left) and the resulting distances at which the traffic aircraft was detected by the test aircraft (right).

Taking an average of the results we arrive at a distance of **1.25 miles or about 2 km** as a typical range at which the traffic aircraft becomes visible to the test aircraft by a pilot. For an AWE situation our `traffic` aircraft is the airborne part of our system which is constantly changing orientation so from that perspective using the average distance is probably conservative.

Furthermore, based on video captured during the flights, the authors could derive a relationship between the detection range and the wingspan of an aircraft by means of a digital camera as shown in the formula below.

$$Range = \frac{HSW \times Wingspan}{OccupiedPixels \times \tan\left(\frac{FOV}{2}\right)} \qquad (5.3)$$

HSW is the **Half Screen Width** in pixels, **FOV** is the **Field of View** of the camera in degrees, and **OccupiedPixels** is the smallest number of pixels once filled with the aircraft image enable it to be detected by a human observer, which was estimated at 17 pixels.

In practice the visible range should be rather proportional to the cross-sectional area of the aircraft that is observable, hence the difference in visible range from different orientations as indicated above. However, assuming that the system is constantly changing its orientation with respect to the observer (as in the case of an AWE system operating in a pumping cycle), the wingspan should serve as a good proxy for this visible range.

From the formula derived above, the authors could estimate the distance at which certain sized aircraft will be visible based on different camera resolutions, as seen in the figures below. As the publication was from 2009, they only considered resolutions up to HD (about 2000 horizontal pixels) which is only about half of that of the current 4K standard.
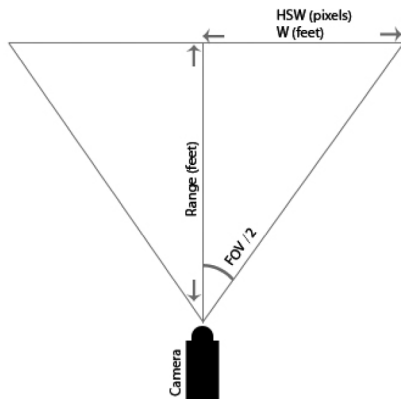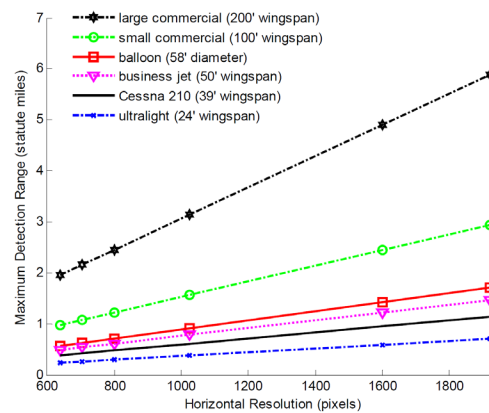
Figure 5.1 - Camera Range Diagram

Figure 5.2 - Range vs. Resolution (Assuming 17 Pixel Minimum Detection Threshold)

Figure 14: Figures from 1. Camera range diagram (left). Detection range vs. camera resolution (right).

The study also determined that the detection distance using the camera was about 2.5 times worse than the mean oncoming detection range for subject pilots performing a visual observation from the cockpit. They also mention the use of an automatic detection algorithm as a possible future development. However, the formulas derived above should still hold with respect to the general relationship between detection range and aircraft size. Using the specifications from a modern camera (DJI Mavic 2 Pro drone camera – specifications described above) the relationships between detection range and wingspan could be calculated as seen in the graph below.

The **OccupiedPixels** parameter from the above formula has been adjusted (from 17 to 13) in order to match the detection range determined in the pilot tests for the test aircraft wingspan (i.e. 2000m for 11m wing span). **This gives a general relationship that the detection range is about 180 times the wingspan of the observed aircraft.**
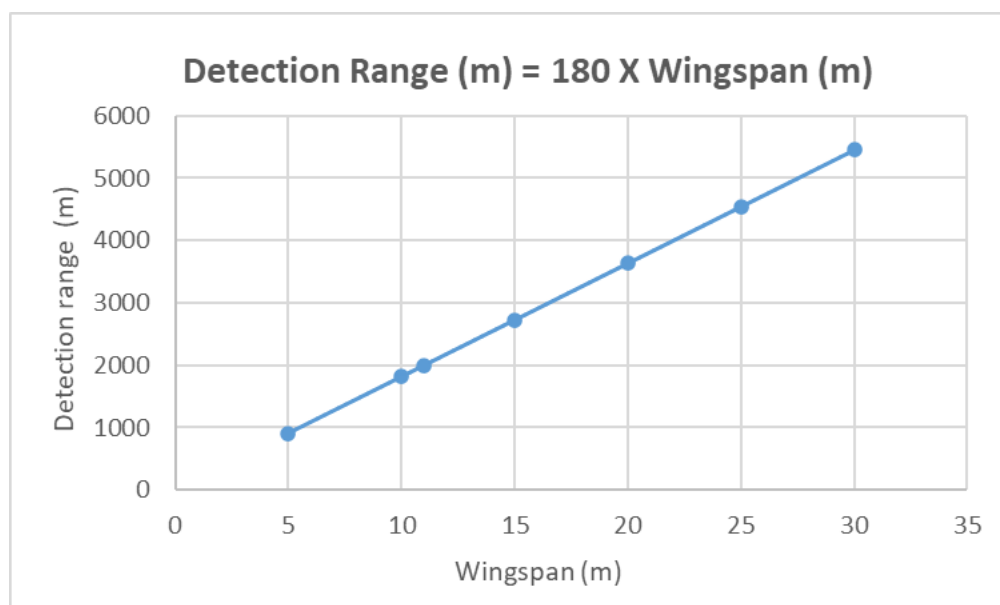

Figure 15: Detection range vs aircraft wingspan based on DJI Mavic 2 Pro drone camera specifications

It should be noted that this relationship is just and approximation and it`s accuracy will depend on many factors such as the sun angle, weather effects, cloud cover, eyesight / attention level of the pilot,… However, it is for sure useful to have a first approximation on which some further analysis can be performed.

From a second study on this topic [2], an estimate of detection and reaction time of 12.5 seconds was estimated for an average person. A breakdown of individual events which would be required to see and then react to an incoming aircraft are shown in the table below.

Table 1

Aircraft Identification and Reaction Time Chart

Event	Seconds
See Object	0.1
Recognize Aircraft	1.0
Become Aware of Collision Course	5.0
Decision to Turn Left or Right	4.0
Muscular Reaction	0.4
Aircraft Lag Time	2.0
TOTAL	12.5

(FAA, 2016b, p. 2)

Figure 16: Table from 2. Breakdown of individual actions needed to observe and react by a pilot.

As a first approximation it is assumed that this estimate would hold for an aircraft pilot who is flying towards an AWE system in operation and must perform a de-confliction maneuver in order to avoid a potential collision. Based on this we can calculate the minimum distance at which an aircraft travelling at a certain speed would need to see an obstacle in order to perform a successful de-confliction maneuver. This has been calculated for a range of aircraft models in the table below.

		Reaction time (s)	12.5
Aircraft	**Cruise speed (knots)**	**Cruise speed (m/s)**	**Min. reaction distance (m)**
Glider (thermalling speed)	50	26	322
Piper PA-28	108	56	694
Pilatus PC-6	115	59	739
Cessna 172	122	63	784
Cessna 182 Skylane	145	75	932
Diamond DA40	151	78	971
Cessna 206	163	84	1048
Cirrus SR22	183	94	1177
Pilatus PC-12	285	147	1833
Pilatus PC-21	370	190	2379
Boeing 737	450	231	2894

Figure 17: Minimum reaction distance calculated for a number of common aircraft models

Combining this minimum reaction distance with the relationship between wingspan and detection range determined above, we can calculate a **minimum avoidable wingspan** for various aircraft as

shown in the graph below. The cruise speeds of the various aircraft models as well as the wingspan of TwingTec`s pilot wing (T29) and product concept TT100 are shown as well.
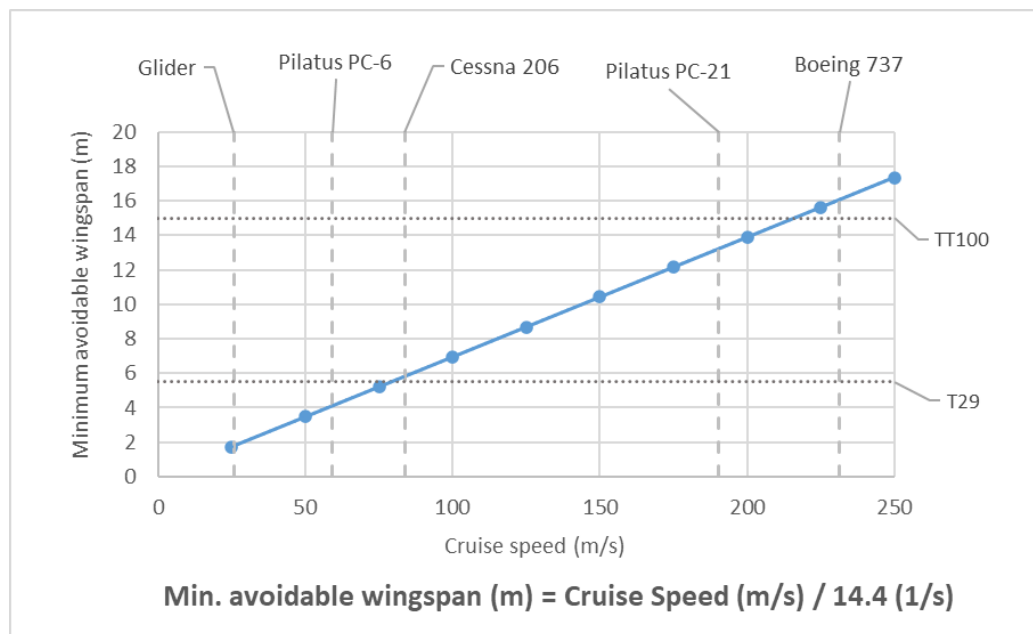

Figure 18: Minimum avoidable wingspan vs. aircraft cruise speed.

From this graph we can identify a generation relationship between the minimum wingspan which would be avoidable by an average pilot vs. the speed of an aircraft. **The minimum avoidable wingspan (m) is equal the cruise speed of the aircraft (m/s) divided by 14.4 (1/s).** This is the factor 180 calculated above divided by the reaction time of 12.5 seconds.

Although this result is just an approximation it gives a good starting point to consider the above calculated detection ranges from an air hazard deconfliction perspective. For example, a Cessna 206 cruising at 163 knots (84 m/s) should be able to see and avoid TwingTec`s pilot system aircraft (T29) which has a wingspan of 5.5m. Based on its wingspan it should be visible from about 1km distance at which point the pilot would need about the same distance to observe it and perform an evasive maneuver.

Based on the same logic, TwingTec`s product concept TT100 with a wingspan of 15m, should be avoidable for a fast plane cruising at 450 knots (231m/s) (e.g. a large commercial airliner like a Boeing 737). The 737 of course not a very relevant comparison as commercial airliners operate well above 10km whereas the TT100 would have a maximum operational altitude of around 300m. Also, the estimate of aircraft lag time would also be significantly larger for such a large aircraft.

However, the PC-21 example is relevant from a Swiss perspective. During tests at one of our test sites we have observed PC-21 training aircraft which have flown over the tests site while we have been there. With a planned wingspan of 15m, the TT100 air vehicle should be visible at a distance of 2.7 km. Travelling at 370 knots (190 m/s) the PC-21 would need about 2.4 km to observe it and perform an evasive maneuver, a buffer of about 300 m. Considering it is a small and highly maneuverable aircraft the reaction time assumption of 12.5 seconds should be relevant.

Considering TwingTec`s product concept TT1000 which is intended to have a wingspan in the range of 30m, it should be visible from about 5.4km. This is about the same (5km) as the visibility requirement for aircraft operating under Visual Flight Rules (VFR) in class G airspace (below 1000 ft AGL – about 300m) which is the type of airspace in which commercial products will be deployed. If the

5km visibility is not possible then the indicated airspeed must be reduced to 140 kts (72 m/s) so anything with a wingspan above 5m (72 m/s / 14.4 1/s) should be avoidable.

<u>Development and implementation of solutions to maximize visibility</u>

Regardless of the distance at which a certain flight object should become visible to the pilot of an oncoming aircraft, it makes sense to implement whatever solutions are possible in order to maximize that distance. During the development of our pilot aircraft (T29) the design team took care to implement all possible solutions in order to make the aircraft as visible as possible. An overview of the marking and lighting scheme, that was implemented can be seen in the figure below.
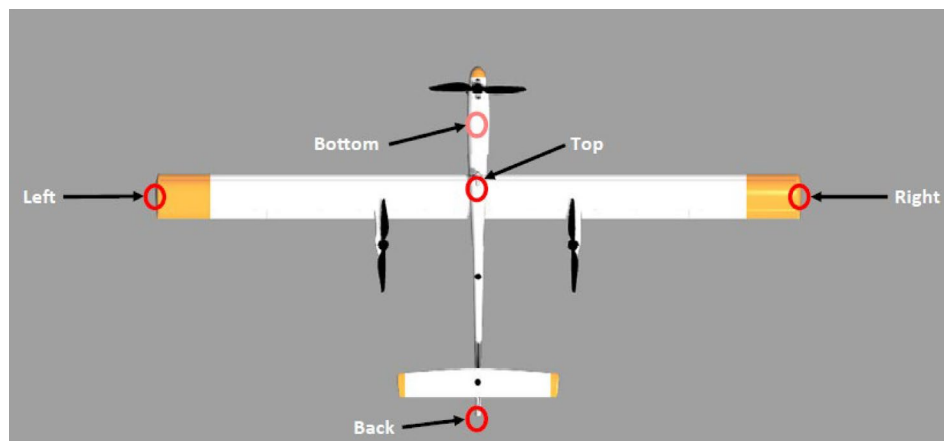

Figure 19: Marking and lighting scheme implemented on T29.

The specification of the paint colors used are shown in the table below. The logic is that the white color is highly visible against a clear blue sky and that the orange color is highly visible against a cloudy backdrop.

Color paint	Paint name	RAL Name	Color Name	Provider
White	Nuvovern ACR	RAL 9010	Pure White	Mäder
Orange	Nuvovern ACR	RAL 2008	Bright red orange	Mäder

The specifications of the lighting system is shown in the table below, procured from the company <u>Innoflyer</u>. Although this lighting system does not have a specific certification (like CS-23) it was the most powerful lighting system that was practically possible to integrate onto the aircraft.

LED Position	LED Name	LED color	Type of blinking	Light brightness	Max Led Current	Provider
Left	Luna Red	Red / White	Red: Always on White: Strobe	Red: 100 lm White: 190 lm	200mA	Innoflyer
Right	Luna Green	Green / White	Green: Always on White: Strobe	Green: 150 lm White: 190 lm	200mA	Innoflyer
Top	Emma	Red	Beacon	Red: 100 lm	200mA	Innoflyer
Bottom	Leila	White	Always on	White: 190 lm	200mA	Innoflyer
Back	Cristal	White	Always on	White: 190 lm	200mA	Innoflyer

After the test flights performed in Feb. 2020, the results of the initial visibility tests were communicated to FOCA along with an overview of the marking and lighting scheme introduced above. In March 2020 we had a call with a number of their personnel and an overview of their feedback as well as some additional action items are listed below.

General feedback from FOCA:

- With its relatively large size (5.5m span) and well visible painting, T29 should improve the visibility for an incoming aircraft. This has been confirmed by the literature study presented above.

- We should check if our lighting system is CS-23 (13.92) compliant, if that is the case then the lighting topic would be sufficiently addressed by using aviation standards. This was further analyzed, see below.

- The visibility of the tether is their main concern, if there is something that can be done to improve this that would be worthwhile. A few ideas were discussed:

    o Put a flag(s) on it. This was further analyzed, see below.

    o Blinking lights on the wing and GS. This concept was adopted by Makani and although will help improve visibility during the nighttime is not expected to help for the current daylight only operations. Not further analysis was performed.

    o On-board FLARM. It was recommended to check with the FLARM supplier if this would help, further details below.

- We should check how the FLARM alert zone warnings distances correlate to the time needed to perform an emergency landing and make sure this is consistent. This point has been further analyzed below.

- The theoretical possibility to register ourselves as an `obstacle` which might be an alternative to putting out a NOTAM. This option has been mentioned but further assessment will be required. FOCA mentioned that the obstacle database in Switzerland is quite dynamic and is updated on a regular basis -> for temporary cranes for example. However, the current regulatory framework sees the system as a UAV following internal assessments.

- FOCA personnel would be happy to join the next tests to get a firsthand impression on the system in operation.

Based on this discussion, four specific action items were identified and investigated, the results of which will now be discussed.

1 – Check for compliance of T29 lighting to CS23

The EASA Certification Specifications for lighting for Normal, Utility, Aerobatic and Commuter Category Airplanes are found in Book 1 (Airworthiness code) Subpart F (Equipment) of CS-23 under the heading LIGHTS on page 1-F-12. The parts of this chapter and their relevance to an AWE application are summarized in the table below.

Furthermore, a GAP analysis has been performed in order to assess to what degree the current lighting system (as presented above) reflects the requirements set forth in CS-23. A summary of this analysis in terms of the compliance of the TT pilot system with these requirements has been included in the last column.

The basic conclusion is that the position lights (forward facing red / green + backwards facing white) should fulfill the specifications for light intensity but not distribution. The anti-collision lights (flashing white on wingtips / rotating red on top and bottom) will not fulfill the specifications for light intensity nor distribution.

Designation CS 23.XXXX	Name of section	Relevant for AWE?	Compliance of TT pilot system with CS 23 requirements
1381	Instrumentation lights	NO	NA
1383	Taxi and landing lights	NO	NA
1385	Position light system installation	YES	Yes, colors and positions of lighting has been implemented as specified.
1387	Position light system dihedral angles	YES	Yes, the position light angles are compliant.
1389	Position light distribution and intensities	YES	Procedures for measuring the light distribution and intensities of positions lights
1391 / 93	Minimum intensities in the horizontal / vertical plane of position lights	YES	Conclusions from supplier: The position lights should fulfil the specification for the light intensity but not the distribution. The anti-collision light will not fulfil the spec for the light intensity nor the distribution.
1395	Maximum intensities in overlapping beams of position lights	YES	Conclusion from supplier: Radiation planes critical for position lights and tail light because optically not precisely defined on the lamp.
1397	Colour specifications	YES	Input from Supplier: Standard not understood, further clarifications needed although compliance is expected.
1399	Riding light	NO	NA

1401	Anti-collision light system	YES	White strobes installed on each wingtip as specified. No rotating beacons installed. For same reason as 1391/93, the anti-collision light will not fulfil the spec for the light intensity nor the distribution.

2 – Check for performance loss to pilot system with a 2m2 flag on the mid-point of the tether

The idea of putting a 2m2 flag (same area as T29) on the mid-point of the tether was also investigated. The intent would be that this could help to improve the visibility of the tether or at least make it obvious that the Twing is connected to the ground so that a pilot does not try and fly underneath it.

This approach would have two major downsides. First of all, it would create additional drag which would reduce the system performance. Second, it would be difficult to implement in practice as the midpoint of the tether needs to reel on and off the winch during the launch and landing process so some sort of de-coupling or sliding mechanism would be needed. The second point is not so obvious and would require some design work, but at least the performance impact from an aerodynamic perspective can be easily investigated and will now be presented.

Aerodynamic drag created by a flag is created by friction of the air passing over the surface (skin friction) as well as the induced drag from the movement of the flag which depends on its aspect ratio (fineness) and weight per area. In general, a higher aspect ratio flag (i.e. longer than it is tall) will have a lower drag coefficient and therefore a lower performance loss.

The parameters which define the aspect ratio of the flag are shown in the figure below. For our example we assume that the length L = 2m and the height l = 1m, giving an aspect ratio of 0.5.
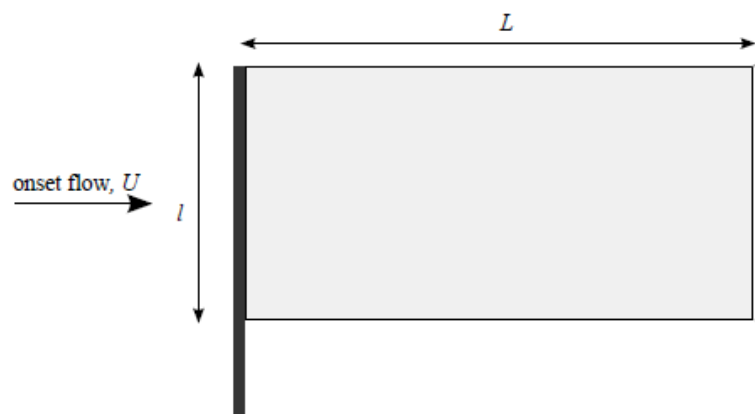
Figure 20: Key dimensional properties of a flag

Although the drag created by a flag in the wind is a relatively complex phenomenon, there are references in literature which can be used like the one shown in the figure below from [3]. This shows a drag coefficient for various aspect ratios and Reynold`s numbers, which is based on the airspeed and a dimensional property – in this case the length of the flag.
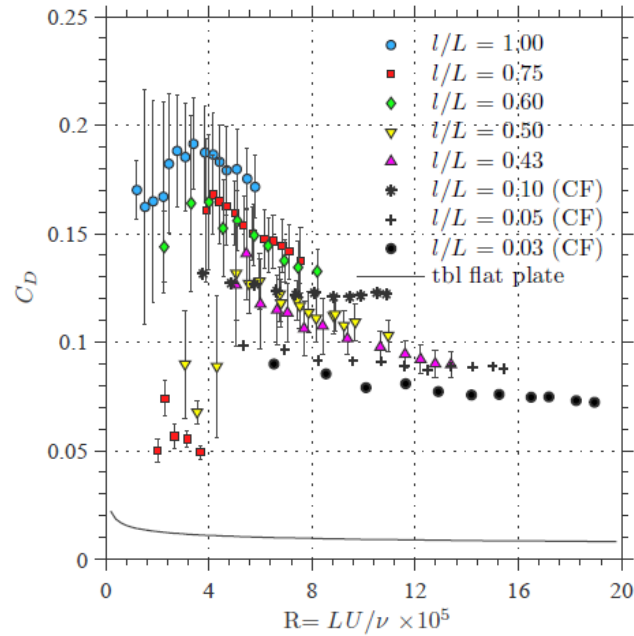
Figure 9: The fluid drag in uniform flow experienced by a horizontal flag. The present measurements for a polyethylene sheet are plotted for five aspect ratios $\mathscr{A} = l/L$ with error bars corresponding to the standard deviation of C_D at each measured flow velocity. Published data (Carruthers and Filippone, 2005), denoted 'CF', for a cotton flag provide three additional values of $\mathscr{A}$. The solid line represents the expected fluid drag of a flat plate experiencing a turbulent boundary layer (cf. Schlichting and Gersten, 2000, eqn. 18.99).

Figure 21: Literature reference for flag drag [3]

For our case we have an estimated airspeed at the flag location of about 15m/s (as it is only at the halfway of the tether, so it does not move as fast as the Twing) and a length (L) of 2m so the Reynold`s Number (R) is calculated as about 20×10^5. Although there is not data for such a high R for our aspect ratio (l/L = 0.5), we can assume that it stays at 0.1, which is probably a conservative value as the drag values are generally decreasing with increasing R.

Drag force is proportional to airspeed squared:

F_D = ½ x rho x v^2 x C_D x A

Airspeed is only 50% at the flag compared to at the Twing (halfway along the tether). Thus the effect of the drag is only 25%. The area of the flag is the same as wing area (2m2 for T29).

Therefore,

CD_total = CD_wing + CD_flag/4 + CD_tether

From this formula, we have estimated the flag drag to be about 6% of the total drag. Based on this we could calculate that at a mid-wind speed site (8.5m/s), the additional drag created by a flag at the mid-point of the tether would reduce the Annual Energy Production (AEP) of the system by about 10%. As AEP is directly related to the revenues a system generation, this would result in a significant economic impact over the lifetime of the project and is therefore not deemed as a viable option. An alternative option to increasing the visibility of the tether has been developed by Makani together with the FAA will be outlined in section 6 of this report.

3 – Check for on-board FLARM pro`s and con`s and make a recommendation on how to proceed

This option was discussed with customer service at FLARM. The feedback was that it would require a custom firmware and there is uncertainty that it would function at all due to the high g-forces and constantly changing orientation of the Twing. Their recommendation was that the current setup with the FLARM on the ground using the alert zone firmware is indeed the best option.

4 – Check emergency landing procedure time and calculate updated FLARM alert zone settings

With T29 we fly on a maximum tether of 350m and our max-reel-in speed of the ground station is set to -3.5m/s when the Twing is in hovering mode. Based on this we can calculate that if the Twing transitioned to hover at its maximum tether length it would take approximately 100 seconds in order to land it, but more like 120 seconds with acceleration and deceleration.

However, in order to avoid an aircraft it is not needed that the Twing goes right to the ground but rather below a certain altitude threshold that would effectively mitigate the risk of a mid-air collision. As per the tethered emergency landing procedures in our CONOPs this altitude is set at 150m, which would still require about 60 seconds based on the values presented above.

For an aircraft travelling at 140 kts (72 m/s) – see discussion at the start of this chapter – and a reaction time of 15 seconds (based on inputs from FLARM (info@flarm.com) and consistent with the values used in the calculations above), this would mean that a pilot would need to make visual contact or be warned (i.e. by their FLARM system) at a distance of about 1km. The alert zone radius has been set to 1.25km in order to give some additional buffer. Although increasing the alert zone radius would give additional time for the pilot to react, it was recommended by FLARM that the alert zone size should only be as large as needed as it is quite stressful for pilots when they get this warning. Based on this a further update of the operational concept was made so that the FLARM system is only active when the Twing is airborne.

Furthermore, this alert zone radius of 1.25km is also very much consistent with the distance at which an aircraft with the wingspan of T29 will become visible to a pilot. Based on the relationship presented in figure 23, this is calculated as 180 x wingspan or 180 x 5.5m = 990m. So in the case that a pilot is entering the alert zone and hears a warning then they should also be able to relatively quickly make visual contact with the Twing and perform an evasive maneuver. Assuming the pilot has read the NOTAM that is published before each test day then the context of the object should also be clear, leading to a good understanding of the danger and a high degree of air risk mitigation.

Dissemination of learnings:

A summary of the key learnings from the project activities with regards to maximizing visibility of AWE system for all airspace users has been included in section 5 of this report, with the 3 key elements:

1 – Marking and lighting.

2 – Use of FLARM with Ground Alert Zone.

3 – Publication of a Danger Zone via NOTAM.

In case these strategic mitigations don`t work then a fourth mitigation (tactical) is also recommended:

4 – Observer and pilot on site.

These recommendations have been published as part of a "Safe AWE Testing and CONOPS guideline" on the Airborne Wind Europe website, links to which have been listed in section 5.

Furthermore, the results have been disseminated to the FGW AWE working group and will be incorporated into the technical guidelines / requirements that are being developed.

Performance measurements with LIDAR:

The data shown in this section is from the test flight in Nov. 2020, in the graph below the tether angles azimuth (horizontal) and elevation (vertical) are shown vs. the line length. From the line length we can see that the system performed 10 pumping cycles. The autopilot was enabled for most of the flight.
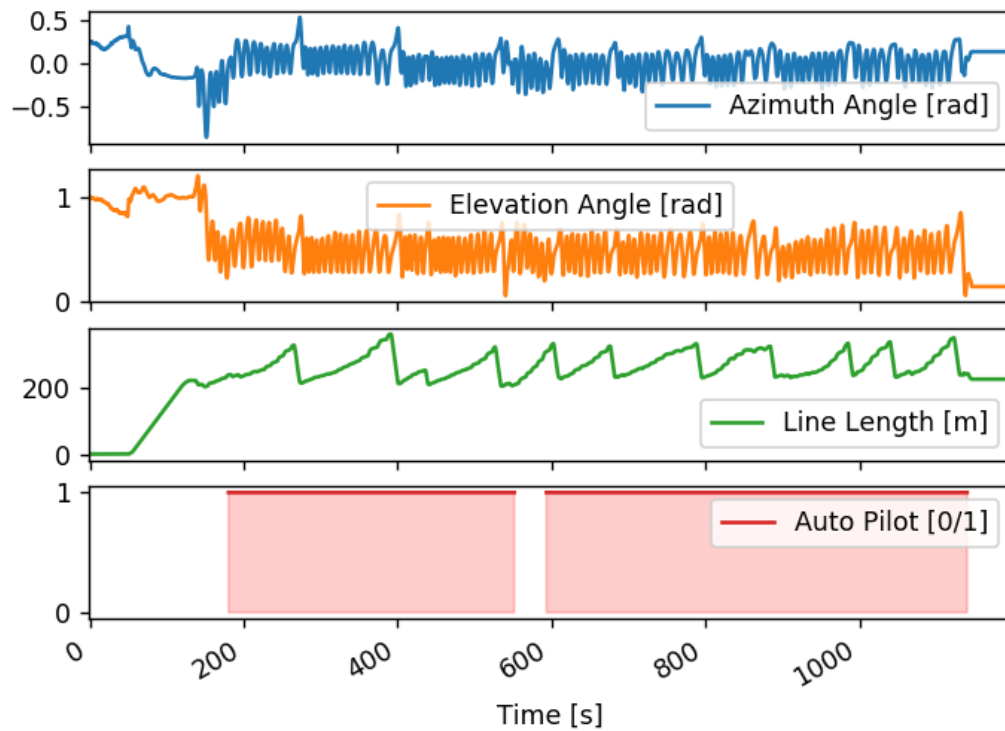

Figure 22: Time series data from test flight.

The plot below shows the mean, max and min wind speed vs. altitude as measured with the LIDAR. The location of the Twing is shown in red, which varies between 50 and 200m during the flight. The process for calculating the wind speed at the Twing location was described previously in section 3. The mean wind speed was calculated over the entire flight time of approximately 20 minutes.
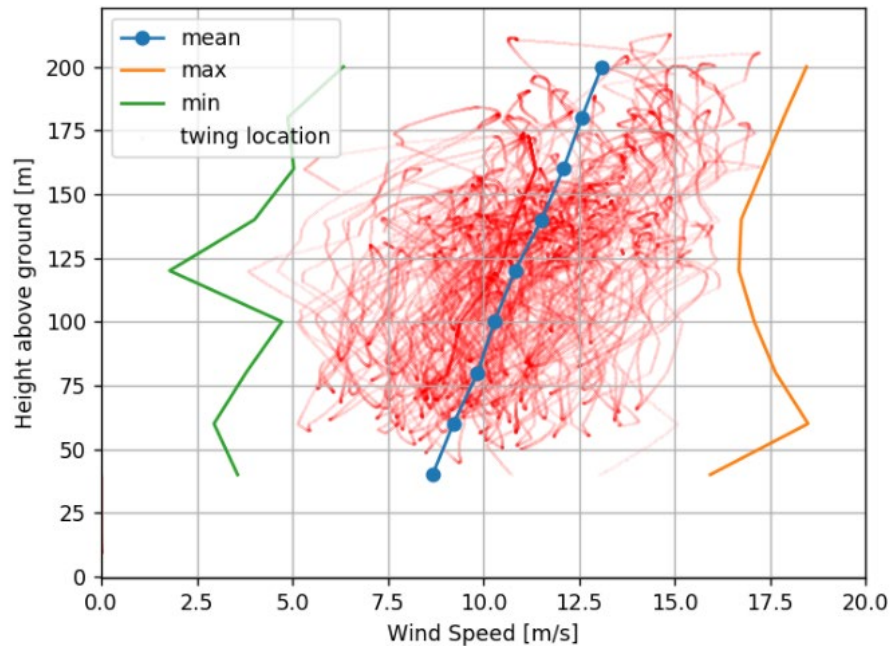
Figure 23: LIDAR wind measurements and Twing Location during test flight

Calculation of minimum standoff distance based on acoustic measurements:

During the acoustic measurement "tow tests" performed with EMPA, two flights were performed at different driving speeds resulting in different wind speeds, resulting in the two different emission spectra shown in the figure below. These plots represent the spectral sound emission of the system averaged over about 100 second, where the Twing was flying crosswind loops (power producing mode). During each loop, the airspeed of the Twing changes and therefore the loudness of the sound also changes.
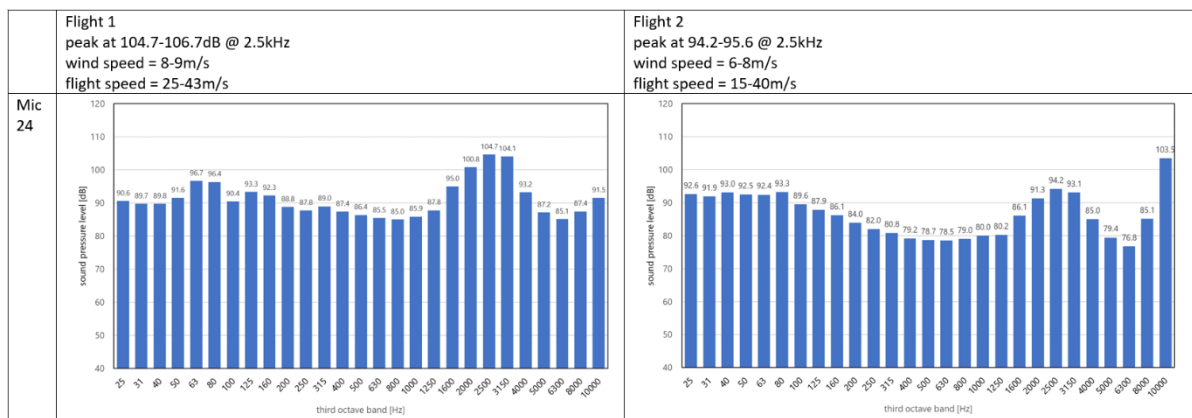

Figure 24: Sound pressure level of system operating during two different flights.

Some general observations can be made from these acoustic profiles:

- A strong audible tonality content can be seen at a narrow-elevated band around 2500 Hz, which can best be described as a whistling sound

- The main driver for the loudness of the noise emissions is the flight speed of the Twing, more details on this will be discussed below.

- The highest frequency bands (6300 Hz and above) are dominated by background noise that is amplified in the inversion of the air damping (i.e. back calculation of emitted sound power accounting for the attenuation of the atmosphere).

Procedure to characterize noise emissions:

In order to calculate the average loudness of the system in operation, we first need to make some assumptions about how often the Twing flies at different speeds. This was done based on our simulation tool, where we can calculate the relationships between airspeed and wind speed as seen in the figure below. As flight 1 was at a higher average airspeed, it should serve as a good representation of the acoustic emissions from the higher wind speed portion of the operational envelope from 9-25m/s. The average airspeed during flight 2 was lower, so should serve as a good representation for the low wind operational envelope from 5-9m/s. It should be noted that this is a relatively rough approximation but based on the experience from the acoustics experts at EMPA, should give a good initial estimate for the overall loudness of the system.
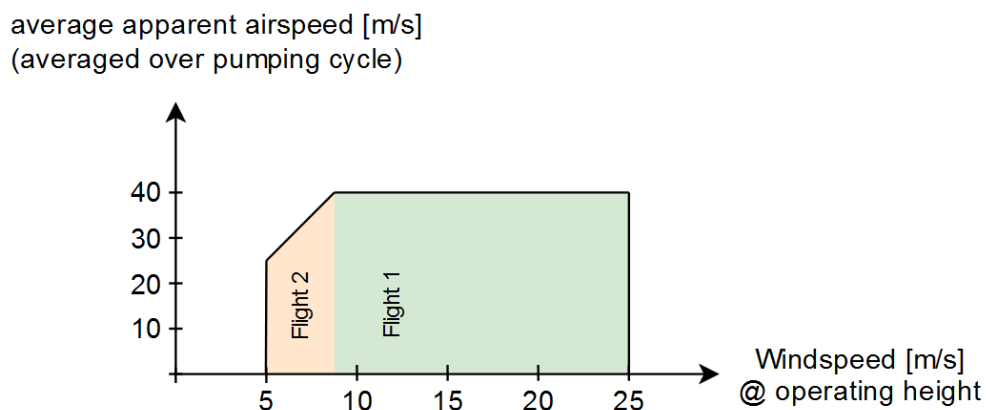

Figure 25: Relationships between airspeed and wind speed.

As a second step we need to make an assumption about how the windspeed changes over time, which of course depends on the site at which the system is installed. For this we can use the wind speed distribution, seen here below (top) for the test site where the wind tests in Feb. and Nov. 2020 were performed. The site has an average wind speed of 5.3m/s at an altitude of 125m above ground level. In order to get a more complete picture, the analysis will also be performed for a higher wind speed site, which is seen on the right in the plot below (bottom) for an average wind speed of 7.5m/s.
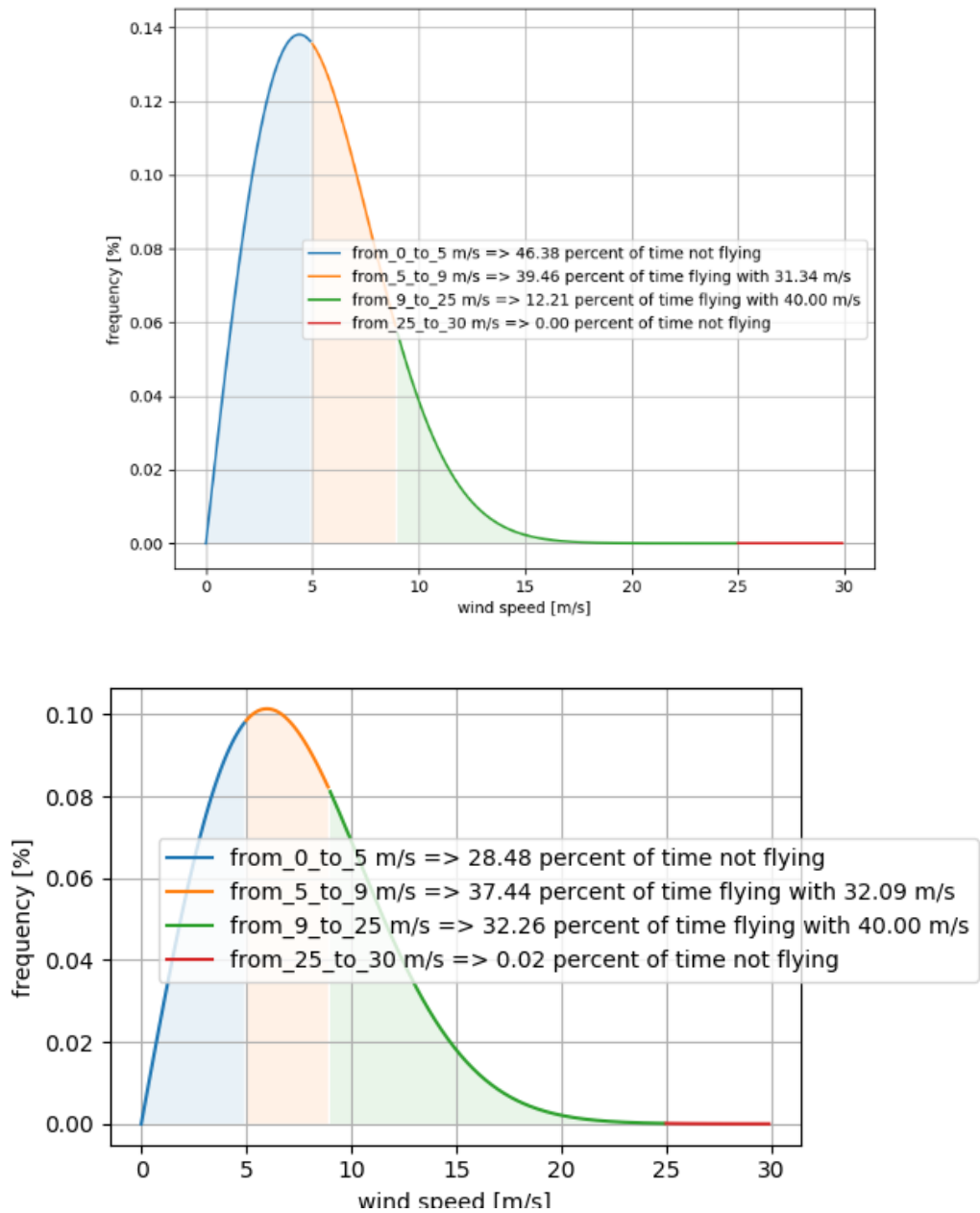
Figure 26: Wind speed distribution for low wind speed site (top) and high wind speed site (bottom)

Apart from the different operating regimes presented above, the Twing also needs to perform a launching and landing maneuver before and after each power production phase which due to the hovering operation has a different acoustic profile. In the figures below, we can see the acoustic measurements for the launching /landing and power production phases as measured in the second flight. During the launching and landing phases (top graph), the airspeed is very low, so the main sound emission comes from the rotating propellers. These are the peaks in the sound pressure level around 100hz, which is consistent with the rotational speed of the VTOL motors.

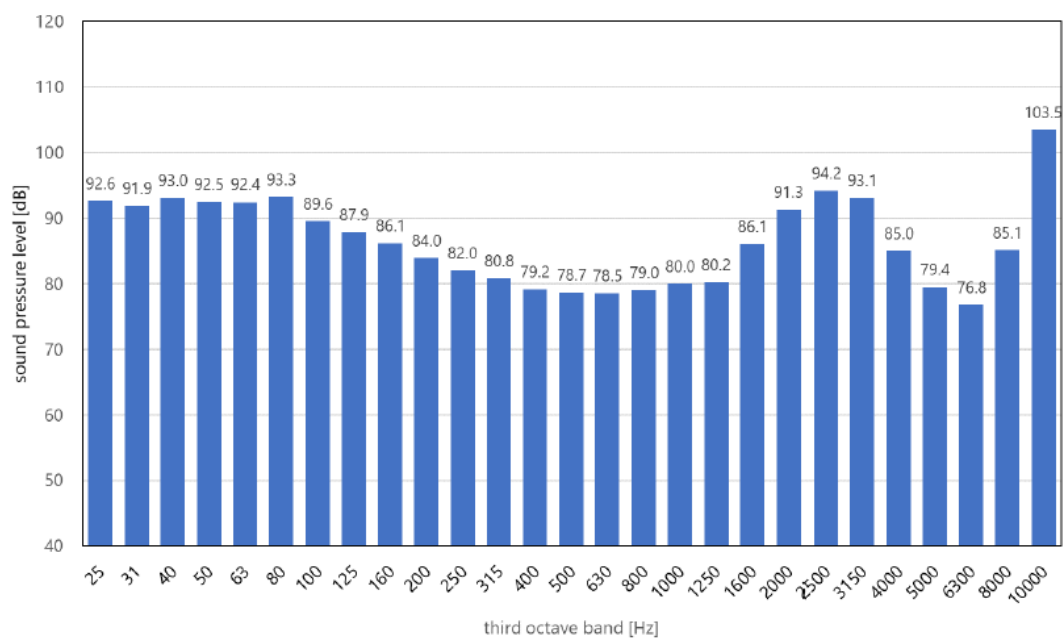## Launching / landing phase:
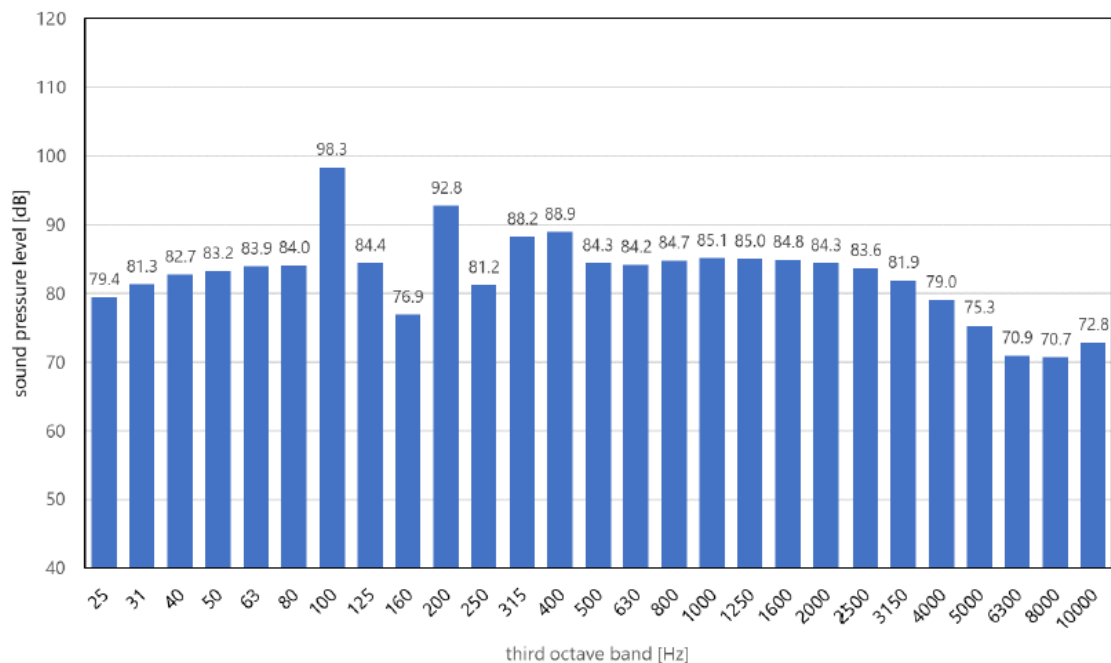
Power production phase:

Figure 27: Acoustic measurement profile from launching/landing and power production phase of flight 2.

As the sound emissions during launch and land are not significantly higher than those during the power production phase, we decided to not include them in the analysis of the standoff distance. Depending on the site, we estimate that the system performs a launching and landing maneuver about 500 times per year, with a duration of about 5 minutes. This means that the system is hovering for about 40 hours per year, compared to around 4000 hours spent airborne, a fraction of only 1%. As the standoff distance is calculated based on the time weighted average sound emissions, the impact of the launching and landing phase is expected to be minimal.

Calculation of the standoff distance:

To get the standoff distance we have to calculate the emission spectra at the receiver position, add the A-weighting and compare the dB thresholds derived in the Swiss Noise Abatement Ordinance (which can be downloaded here).

A-weighting is applied to instrument-measured sound levels to account for the relative loudness perceived by the human ear, as the ear is less sensitive to low audio frequencies. The effects of this can be seen in the figure below for the first flight. First the sound pressure level at 1m from the Twing is calculated, accounting for the effects of air absorption, this gives the blue bars. Then the A-weighting is applied, which adjusts for the frequency dependence of the human ear, giving the red bars.
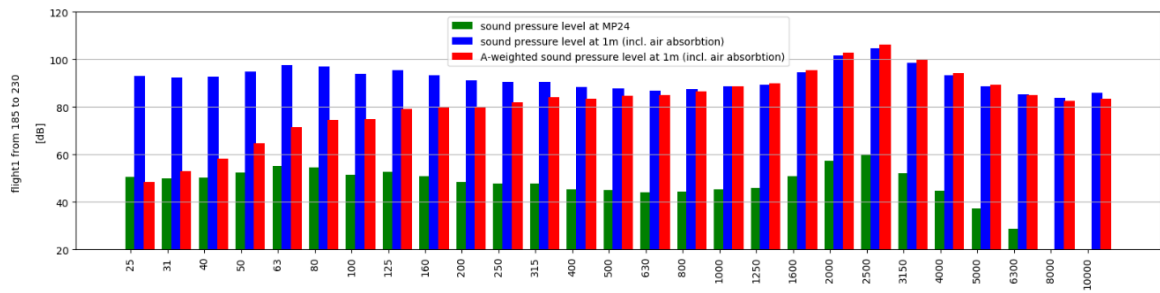

Figure 28: Calculation of A-weighted sound pressure level at 1m from microphone measurements.

For a set of discrete distances (D), the following calculation steps have to be done for each frequency of both emission spectra:

1) Calculating the spectral Sound Power Level (SPL) at the receiver position.

$$SPL_{Xm} = SPL_{1m} - 20 * log(D) - A_{atm}[f] * D - A_{gnd} + A_{weight}[f]$$

This includes:
   a. The inverse distance law, the sound pressure (SPL) decreases with distance from the sound source
   b. Air absorption for each frequency (f)
   c. A correction for reflection of soundwaves at the ground
   d. A-Weighting for each frequency to account for the relative loudness perceived by the human ear

2) Calculate dB(A) from one-third octave band sound pressure levels.

3) Calculate Leq by respecting temporal dilution which was derived from the wind speed distribution and system operation characteristics

$$Leq = 10 * log(0.39 * 10^{SPL_{Flight2}/10} + 0.21 * 10^{SLP_{Flight1}/10})$$

4) Add correction terms to find the rating level Lr

$$Lr = Leq + K1 + K2 + K3$$

These coefficients are selected from three different tables in section 33 of the noise abatement ordinance. These are first estimates based on input from the acoustic experts at EMPA, but have not yet been confirmed by a regulatory authority.

K1.a = 5, for industrial, commercial and agricultural installations, giving a 5 dB penalty.
K2.d = 6, for strongly audible tonality content, giving a 6 dB penalty.
K3.a = 0, for non-audible pulse content.

5) And finally compare the resulting Lr for the different distances with the thresholds from the Exposure Limit Values for Industrial and Commercial Noise table in Annex 6.2 of the noise abatement ordinance.

These values are shown in the table below and indicate that the threshold for our system would be between 45 and 60 dB, depending on the sensitivity level of the area and if it is day or night. As wind speeds are typically higher during the nighttime hours, we have decided to use the nighttime values, which would be a bit conservative.

Sensitivity level (Art. 43)	Planning value Lr in dB(A)		Impact threshold Lr in dB(A)		Alarm value Lr in dB(A)	
	Day	Night	Day	Night	Day	Night
I	50	40	55	45	65	60
II	55	45	60	50	70	65
III	60	50	65	55	70	65
IV	65	55	70	60	75	70

Sensitivity Level	Description
I	Zones with higher noise abatement requirements, notably in leisure zones.
II	Zones in which operations that emit noise are not permitted, notably in residential zones and zones for public buildings and installations.
III	Zones in which operations emitting a certain level of noise are permitted, notably in residential and industrial zones (mixed zones) and agricultural zones.
IV	Zones in which operations emitting a high level of noise are permitted, notably in industrial zones.

Figure 29: Threshold values from Annex 2.6 of the Swiss Noise Abatement Ordinance (top). Description of sensitivity levels from Art. 43. (bottom)

From the intersections of the partial rating sound level (Lr) and the thresholds for the different zones, we can calculate the range of standoff distances, as seen in the figure below. For the test site, with an average wind speed of 5.3m, the standoff distances would range from 288m to 780m. **It is expected that this would be a zone 3 site as it is a rural area with agricultural usage, so the standoff distance would be in the range of 400m.**

Although it is just an approximation, we can assume that this distance would be measured from the Ground Station (GS) location. In reality much of the sound emissions would come from the Twing, which operates some hundreds of meters away from the GS in a downwind direction. But if we assume that there is not a single prevailing wind direction then this effect should cancel itself out.
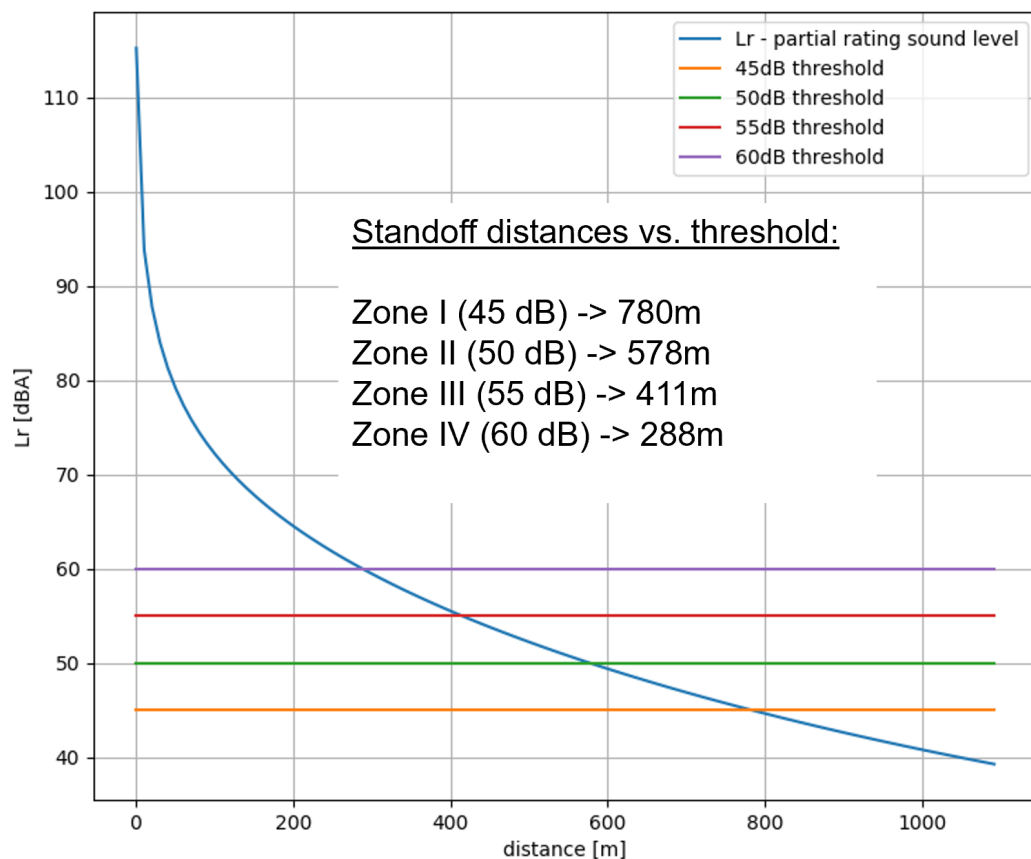

Figure 30: Standoff distances vs. noise thresholds / zones for low wind site.

The standoff distances per zone are calculated for the high wind (7.5m/s average) below. **For the zone 3 case, the distance would increase by about 100m due to the increased frequency of operation.**
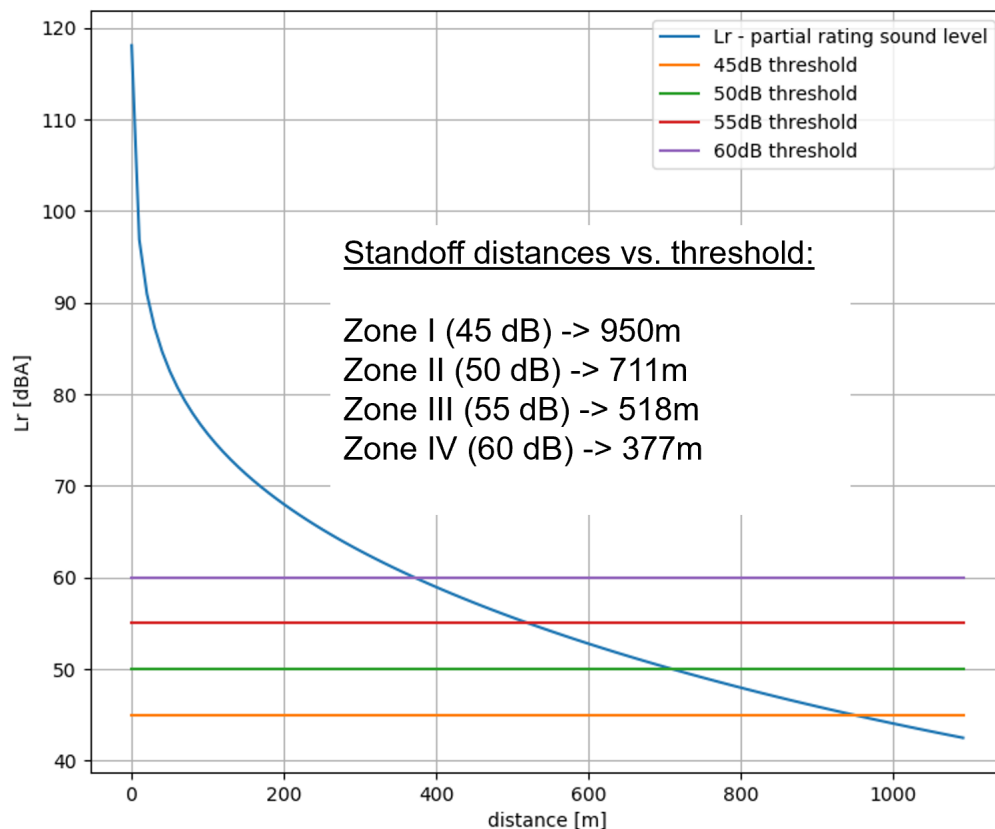
Figure 31: Standoff distances vs. noise thresholds / zones for high wind site.

Improvement potential of the calculation scheme:

The accuracy of the calculation scheme could be improved in two main ways:

1 – Characterize the site in more detail.

- Take into account the time variation in the wind speed so that the impact of night vs. day thresholds could also be captured.

- Consider the directional dependency of the wind (as previously mentioned) which will influence the location of the Twing over time. The Twing always flies downwind from the ground station at a certain tether length, and as the Twing is the main source of the emissions this means the resulting standoff distance would not be a circle around the ground station but rather have a more complex shape which could be relevant in a siting analysis.

2 – Use a finer discretization of the emission spectra by filtering the data and mapping the frequency spectra into flight speed `bins`, say of 1m/s. This would allow for the calculation of a more accurate relationship between average wind speed and sound power level. Alternatively, the emission spectra could be characterized based on the instantaneous airspeed of the Twing, and then the average noise levels calculated based on a flight simulation.

5   Conclusions

Visibility of AWE systems for airspace users

An AWE specific approach to air risk mitigation in the testing and demonstration phase has been developed and evaluated through the project activities. This is based on four key elements:

1 – Marking and lighting: In order to make the system as visible as possible to incoming air traffic the use of appropriate marking and lighting is recommended. Marking should consist of at least two colors, white which is highly visible on the backdrop of a blue sky and orange / red which is visible on a cloudy backdrop. The use of high-power LED lighting (whatever is possible to be practically integrated onto the aircraft) is also recommended, with colors according to aviation standards like CS-23. Furthermore, the use of blinking (strobe) lights is also recommended as they help to capture the attention better than a continuous light. An updated lighting and marking specification have been prepared for TwingTec's pilot aircraft. A GAP analysis has been performed to check what parts of CS-23 the current lighting system can satisfy.

2 – Use of FLARM: FLARM is a radio-based collision avoidance system for manned and unmanned aircraft and is widely used in Switzerland and Europe. Although typically mounted on the aircraft it is also possible to be used on the ground with a special firmware called "Ground Alert Zone". This broadcasts a danger zone which alerts incoming aircraft which are equipped with FLARM that there is a specific danger ahead (at the warning limit for incoming), and the user is also warned of incoming aircraft (at the incoming warning limit). However, since not all aircraft are equipped with FLARM, further means to assure tactical mitigations should be considered, as appropriate. Recommended settings for the alert zone parameters are shown in the table below:

Alert Zone Configuration Parameters:	Radius (m)	Height (m)
Incoming warning limit	4,500	1,000
Warning limit for incoming	1,250	500

3 – Publication of Danger Zone via NOTAM: The publication of a Danger Zone (TEMPO D-AREA) via NOTAM (Notice to Airmen) is performed prior to any flight tests based on the current authorizations from FOCA, which mandates this. In theory this should warn pilots that there is a danger to air traffic at the test location (Tethered drone tests in our case) and they should stay clear of the area. However, it must be considered, a Danger Area is not restricting other users from entering it and is only an awareness mean that something potential dangerous is ongoing in this area.

4 – Observer and pilot on site: Based on our current Operational Approval from FOCA it is required that we have an observer and a pilot on site during operation. This is a typical requirement for UAV operations in the specific category and we have adopted it as a tactical air risk mitigation strategy. The purpose of the observer is to keep an eye out for incoming aircraft by both visual and electronic means (i.e. using the FLARM system). If an incoming aircraft is approaching and the observer determines that there is a chance that it is on a collision course and does not recognize there is an air risk present, then he/she signals to the pilot of the tethered drone to initiate an emergency landing. This is of course not a viable option for commercial operations, some outlook on this will be shared in section 6.

The recommendations described above have been published as part of a "Safe AWE Testing and CONOPS guideline" on the Airborne Wind Europe website:

https://airbornewindeurope.org/working-group-awe-safety-and-technical-guidelines/

https://airbornewindeurope.org/wp-content/uploads/2021/02/AWEurope_Safe-AWE-Testing-CONOPS-Guidelines_V1.1_v2020-01-25.pdf

Further details and considerations regarding the Specific Operation Risk Assessment (SORA) process have also been published:

https://airbornewindeurope.org/wp-content/uploads/2021/02/AWEurope_Introduction-to-SORA-for-AWE_V1.1_v2020-01-25.pdf

Before publication these guidelines were reviewed by Swiss FOCA and were also presented at the airborne wind energy conference in Glasgow in 2019:

https://www.awec2019.com/awec2019_program.pdf

Performance Measurements

Wind tests with a LIDAR were performed, the following conclusions can be drawn:

- Wind speed at Twing during flight operations can be calculated from the 1Hz LIDAR measurements, but has some limitations in terms of capturing turbulences smaller than about 200m.
- Tow tests remain the best method for the validation of system performance and for model validation due to the controlled wind field.
- Augmentation of both techniques with high-quality on-board sensing of airspeed, AOA and sideslip are recommended for further measurements.
- LIDAR can be used for quantification of power output with sufficiently large datasets using averaging times of 10 minutes or cycle based averaging which is recommended.

Acoustic characterization

- The emission spectra of the system in its various operational modes (launching, power production and landing) could be measured during a tow test.
- A correlation between the flight speed of the Twing and the noise emissions generated was identified.
- The noise emissions during launching and landing are not significantly higher than those during power production. As a commercial system would only spend about 1% of its operational time launching and landing, compared to 99% in power production, the launching and landing phase is therefore negligible in the calculation of a standoff distance.
- The standoff distance depends on both the average wind speed at the site as well as the sensitivity class of the location. For a sensitivity class 3, which is estimated to be most relevant for commercial AWE installations, the standoff distance has been evaluated from 400 to 500m (about 1.5 times the max. tether length), for a low and medium wind speed site respectively.
- More research is needed to better understand how the noise is generated, how it is influenced by system scale and how it can be reduced.

6 Outlook and next steps

Looking forwards to a subsequent demonstration project and eventually to commercial operations a number of topics still need to be addressed with regards to the project activities and scope.

Visibility of AWE systems for airspace users

Future development efforts in the context of safe airspace integration will be focused on at least these three topics:

1 – Marking and lighting requirements for commercial demonstrator and product. As a starting point for considering next steps on this topic, the learnings from Makani should be considered. These are summarized in Part 3 of the Energy Kite Technical Report (pages 353 – 368). [4.c] Included is an overview of their interactions with the FAA as well as the final marking and lighting requirements for their M600 test system, a picture of which operating during the night is shown in the figure below left. In the figure below right, an overview of the M600 Energy Kite in its offshore configuration is shown. Here the marking scheme for the wing and tether developed in cooperation with the FAA and approved by aviation authorities in Norway (where this system was operated) is visible.
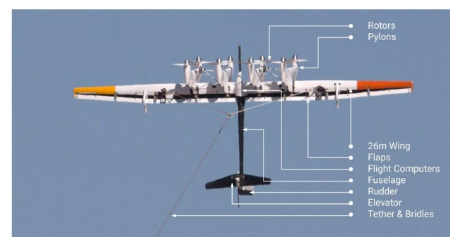

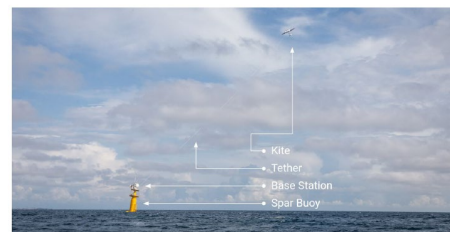Figure 1: Airborne components of an M600 Energy Kite.

Figure 2: M600 Energy Kite flying crosswind loops offshore.

Figure 32: A long-exposure photograph of the Makani M600, SN4 "Lanakila," in night flight at test site in Hawaii. (left) Overview of M600 Energy kite in offshore configuration at test location in Norway. (right) [4.a]

The final requirements for operation based on the FAA DETERMINATION OF NO HAZARD TO AIR NAVIGATION FOR TEMPORARY STRUCTURE issued on 12/13/2019 for operation at test site in Hawaii are as follows:

- Notice to Airmen (NOTAM) issued during operation
- No Temporary Flight Restriction (TFR) required
- Marking:

- o Wing: conspicuous colors
- o Base station: white
- o Tether: alternating 150-foot (45m) bands of white and aviation orange
  - Lighting:
    - o Kite: four enhanced hemispherical ACL strobes
    - o Base station: L-865
    - o Tether: none
- Nighttime operation permitted

Interesting is that essentially the same marking and lighting scheme was accepted by the Norwegian aviation authorities for testing the M600 at the offshore location. This application and some further details about the marking and lighting requirements are included in [5]. Based on feedback from the Swiss FOCA, it is very helpful that such requirements have been established in cooperation with other aviation authorities like the FAA. During the development of a larger scale demonstration system the adoption of these marking and lighting specifications will be investigated in consultation with the relevant authority.

2 – U-space integration. According to FOCA`s website:

The term U-Space (referred to as "unmanned aircraft system traffic management [UTM] in the US), refers to a collection of digitalised and automated functions and processes aimed at providing safe, efficient and fair access to airspace for the growing number of civilian drone operations. U-Space provides a framework to facilitate the implementation of all types of operation in all classes of airspace and all types of environment, while ensuring an orderly coexistence with manned aviation and air traffic control.

The potential for leveraging U-space for integration of AWES was explained in an article published on SUSI website on 23rd of November 2020 here. SUSI stands for "Swiss U-Space Implementation", a Public-Private Partnership launched in December 2018 between FOCA, the Swiss Air Navigation Provider skyguide and a varied range of market players from the industry.

"The U-Space architecture will give more possibilities to deal with specific operations, such as of AWES, by increased automation and efficient data sharing" Perca describes AWES as a "dynamic operation" meaning that they are dependent on real-time weather conditions in order to operate. Furthermore, the usage of remote identification and other services within U-Space, would guarantee a more sustainable, safe and flexible usage of the airspace while supporting the use-case of AWES, as she highlights. Therefore, AWES would be connected to the whole network of interconnected devices, taking advantage of the information provided by the USSPs in the U-Space ecosystem.

As U-space and the associated services are further developed and rolled out throughout Switzerland and Europe, their applicability to AWE systems will be investigated and adopted where possible. It is expected that this work will be performed in consultation with the Swiss FOCA, EASA as well as other civil aviation authorities (where testing and demonstration activities will be performed) as well as other Airborne Wind Energy developers, likely through the AWEurope industry group or as part of FGW guideline development.

3 – Classification of AWE systems as an obstacle / obstruction. From a Swiss / European context, AWE systems are considered as tethered drones and are generally required to operate in the specific category with risks assessed by the SORA methodology. However, in some countries, like the US, they are considered as obstacles or obstructions like a radio tower or conventional wind turbines.

During a discussion with representatives from the Swiss FOCA, they mentioned that it might theoretically be possible to try and classify AWE systems as an obstacle / obstruction in Switzerland

as well, using the obstacle database to notify airspace users of the location and height above the ground. However, this is not straightforward and several items would still need to be clarified (e.g. time limitation, different requirements for markings of obstacles than for aircraft). This brings up an interesting discussion from a legal point of view as when classified as an obstacle, it could be that the requirement to `see and avoid` other airspace users of an AWE system is relaxed or removed all together. For commercial operations this is a very important consideration, as the implementation of an automated `detect and avoid` system could be prohibitively expensive. Under the current specific requirements, we need to have an observer and pilot on site who can fulfill this see and avoid requirement, which is also considered as a no-go for future commercial operations.

For the current testing and demonstration phase, where we will anyways have personnel on site and the number of flight hours are limited, operation under the specific category is acceptable, but for longer term demonstrations and eventually commercial operations the classification as an obstacle / obstruction should be investigated.

Performance measurements and acoustic characterization

1 – Performance validation of AWE systems. Extensive post processing using a model based fitting approach was performed for data collected from both tow and wind tests. Although a LIDAR system was used to capture wind data over a range of altitudes during the wind test, the overall dataset was of limited use from a performance validation perspective. The tow test data, in which the wind field is controlled by the speed of the towing vehicle, was very useful for performance validation and could be used for the validation of our simulation tool. This is important as the simulation tool is used to predict the performance of larger systems on which our future business model and investment case is based.

In order to improve the level of validation as well as the overall understanding of performance the use of on-board measurements of airspeed, side slip and angle of attach are recommended. Although such sensors were installed on our pilot Twing T29 during the test flights, the quality of the sensors and their output data was not so high. Further investigations into higher quality sensors and associated calibration techniques should be performed as part of future activities.

2 – Power curve measurements with LIDAR. Some initial learnings into this topic were generated during the project. The main conclusion is that significantly larger datasets are needed in order to get a better idea about how the power output changes with wind speed and that the averaging times should be synchronized with the pumping cycle operation to avoid measurement artifacts. As there are many degrees of freedom that can be controlled by the autopilot software, such as elevation angle, loop radius, pumping length, aircraft trimming,… the power measurements are always going to depend highly on how well the autopilot is functioning.

Once the pilot system has been further developed and the functionality of the autopilot software has converged, further wind tests with LIDAR will be carried out. These should be performed at a time where the system can operate for many hours in order to collect sufficient data for a complete understanding of the systems power curve.

3 – Noise emissions at larger scales and reduction strategies. From the acoustic measurements performed during tow tests we learned that more research is needed to understand how the noise is generated and how it changes with scale. This motivates the fact that aeroacoustics will be an important subject to further investigate during the design phase of the commercial demonstrator and first products. Getting an in depth understanding of the physical mechanisms which create noise on

the system, how they are impacted by upscaling and most importantly how the acoustic emissions can be reduced will be highly important in order to ensure that the market potential for AWE systems is not limited due to excessive standoff distance requirements.

7 National and international cooperation

During the course of the project we have cooperated with a number of other AWE OEMs and stakeholders through the AWEurope industry group activities as well as the FGW working group on technical guidelines.

8 Communication

During the course of the project, a number of news articles have been published about TwingTec which can be found on our website News Page, links to a few noteworthy mentions are included below:

https://twingtec.ch/2020/03/30/wind-energy-2-0-has-been-awarded-the-solar-impulse-efficient-solution-label/

https://twingtec.ch/2020/12/18/2020-in-review-flight-testing-of-our-pilot-system-2/

https://twingtec.ch/2021/04/22/happy-earth-day-everybody/

9 Publications

Rolf Luchsinger et al. TwingTec's roadmap from full proof of concept to the first commercial product. Book of abstracts of the International Airborne Wind Energy Conference (AWEC 2019).

Corey Houle et al. Safe testing of airborne wind energy systems. Book of abstracts of the International Airborne Wind Energy Conference (AWEC 2019).

AWEurope safety guidelines – see section 5.

10 References

All references made in the report can be downloaded via links in the list below.

1. Master thesis: Comparison of See-and-Avoid Performance in Manned and Remotely Piloted Aircraft.pdf

2. Journal of aviation paper: Seeing the Threat Pilot Visual Detection of Small Unmanned.pdf

3. Paper on Flag Drag topic: Experiments_on_the_stability_and_drag_of_flexible_sheet_Morris-Thomas.pdf

4. Makani Energy Kite Technical Reports:

    a. Makani_TheEnergyKiteReport_Part1.pdf

    b. Makani_TheEnergyKiteReport_Part2.pdf

    c. Makani_TheEnergyKiteReport_Part3.pdf

5. Makani Application to Norwegian CAA for Offshore testing of M600.pdf

11 Appendix